International Journal of Technology 11(1) 26-36 (2020)
Received July 2019 / Revised December 2019 / Accepted January 2020

International Journal of Technology

http://ijtech.eng.ui.ac.id

# Effect of Fuels on the Physicochemical Properties and Photocatalytic Activity of Bismuth Oxide, Synthesized using Solution Combustion Method

Yayuk Astuti[1*], Darul Amri[1], Didik S. Widodo[1], Hendri Widiyandari[2], Ratna Balgis[3], Takashi Ogi[3]

[1]*Chemistry Department, Faculty of Sciences and Mathematics, Diponegoro University, Jl. Prof. Soedharto, S. H., Tembalang, Semarang, Central Java 50275, Indonesia*
[2]*Department of Physics, Faculty of Mathematics and Natural Sciences, University of Sebelas Maret, Jl. Ir Sutami No.36A, Jebres, Surakarta, Central Java, 57126, Indonesia*
[3]*Department of Chemical Engineering, Faculty of Engineering, Hiroshima University, Japan, 1-4-1 Kagamiyama, Higashi*-Hiroshima, Hiroshima*, 739-8527, Japan*

**Abstract.** The potential of bismuth oxide ($Bi_2O_3$) as a photocatalyst, due to its a wide band gap (2.3-3.3 eV), was successfully synthesized using the solution combustion method with several fuels: urea, glycine, and citric acid. The synthesis was started by dissolving bismuth nitrate pentahydrate in nitric acid and then adding the fuel. The solution formed was heated for 8 h at 300°C. After heating, calcination was carried out for 4 h at 700°C. The resulting three products were in a yellow powder form. Fourier Transform InfraRed (FTIR) spectra of the samples confirmed that $Bi_2O_3$ had formed, as indicated by the functional groups of Bi-O-Bi observed at approximately 830–850 $cm^{-1}$ and Bi-O at 1380 $cm^{-1}$. X-ray diffractograms indicated that $Bi_2O_3$ synthesized using urea and glycine fuels was present in the mixed phases of α-$Bi_2O_3$ at 2θ of 27.7, 33.3, 27.2 and β-$Bi_2O_3$ at 2θ of 30.5, 41.8, 45.5, based on the Joint Committee on Powder Diffraction Standards **(**JCPDS) database 41-1449 and 27-0050, respectively. However, $Bi_2O_3$ produced by citric acid fuel comprised only α-$Bi_2O_3$. Furthermore, different fuels produced different crystallite product sizes; urea generated the smallest crystallite, followed by glycine and citric acid. Additionally, the photocatalytic activity on the degradation of methyl orange of $Bi_2O_3$ synthesized using urea fuel exhibited better photocatalytic activity than the other products, with degradation rate constants of $4.38\times10^{-5}$ $s^{-1}$, $3.38\times10^{-5}$ $s^{-1}$, $2.33\times10^{-5}$ $s^{-1}$ for bismuth oxide synthesized by urea, glycine, and citric acid, respectively.

***Keywords:*** Bismuth oxide ($Bi_2O_3$); Photocatalytic activity; Photocatalyst; Solution combustion

## 1. Introduction

Bismuth oxide ($Bi_2O_3$) is a semiconductor that has attracted considerable attention because it exhibits good optical and electrical properties, such as a wide band gap of 2.3–3.3 eV (Hashimoto et al., 2016), high refractive index (n$\delta Bi_2O_3$ = 2.9), high dielectric permittivity (εr = 190), and good photoconductivity (Bedoya Hincapie et al., 2012). These properties have led to the use of $Bi_2O_3$ for the development of gas sensors, anti-reflection coatings, photo-voltaic cells, fuel cells, and optoelectronic devices (Jalalah et al., 2015). In addition, among the active photocatalysts such as titanium dioxide ($TiO_2$)

*Corresponding author's email: yayuk.astuti@live.undip.ac.id, Tel.: +62-21-7560922; fax: +62-21-7560926
doi: 10.14716/ijtech.v11i1.3342

(Rahman et al., 2018) and ZnO (Winatapura et al., 2016), $Bi_2O_3$ has been demonstrated to be a valuable alternative photocatalyst due to its direct band gap energy.

It has been observed that the chemical and electrical properties of $Bi_2O_3$ depend on the synthesis procedure (Gotić et al., 2007). Therefore, careful selection of a synthesis method is necessary. Various techniques have been introduced to synthesize $Bi_2O_3$, including sol-gel (Mallahi et al., 2014), precipitation (Astuti et al., 2017), hydrothermal treatment (Liu et al., 2011), chemical deposition (Cheng and Kang, 2015), and solution combustion (La et al., 2013, Astuti et al., 2019). Most of these methods require high temperatures, long reaction times, or a particular instrument, which are inefficient from the point of view of energy consumption, production cost, and time.

Contrary to other methods, the solution combustion method offers a time-, energy-, and cost-efficient process and a simple experimental setup (Li et al., 2015). This method is based on an exothermic redox reaction between the fuel and oxidant, which generally provides the energy for the metal oxides' formation (Lackner, 2010). Another benefit of this method is the exothermicity of the self-sustaining chemical reaction that drives the reaction because of the presence of the oxidant and fuel (Li et al., 2015).

The effect of various fuels on the solution combustion method has been studied in the synthesis of metal oxides, such as aluminum oxide ($Al_2O_3$), nickel (II) oxide NiO (Raveendra et al., 2016), and $TiO_2$ (Rasouli et al., 2011). These studies reported that the fuels affected the products' physicochemical properties; including morphology, crystallite size, crystalline phase, and crystal system. Urea, glycine, and citric acid are the most commonly reported fuels because of their high exothermicity and ability to coordinate with nitrates (Li et al., 2015). Synthesis of $Al_2O_3$ using glycine resulted in amorphous phase particles, while the use of urea generated crystalline $Al_2O_3$. However, in the case of $TiO_2$ and NiO synthesis, the use of either urea or glycine produced crystalline phase particles, and only $TiO_2$ synthesis using citric acid required further calcination. Regarding morphology, the use of glycine produced particles with higher porosity compared to urea and citric acid, which occurs because of the fuels' molecular structures. Urea, glycine, and citric acid contain amino ($–NH_2$) groups, amino and carboxyl (–COOH) groups, and hydroxyl (–OH) and carboxyl (–COOH) groups, respectively. The order of reactivities of the functional groups from highest to lowest is amino, hydroxyl, and carboxyl, respectively (Li et al., 2015). Even though the importance of fuel type on metal oxide synthesis has been demonstrated, the effect of fuel reactivity on the synthesis of $Bi_2O_3$ using the solution combustion method has never been reported. Therefore, this research aims to investigate the effect of fuels on the physicochemical properties and photocatalytic activity of $Bi_2O_3$ synthesized using the solution combustion method.

In this study, the effects of the reactivities of urea, glycine, and citric acid, as fuels, on the physiochemical properties of $Bi_2O_3$ were investigated. The fuels' influence on the structural characteristics of $Bi_2O_3$ was also evaluated, and the photocatalytic activity of the synthesized $Bi_2O_3$ was measured using dye degradation.

## 2. Methods

### *2.1. Materials*

Bismuth nitrate pentahydrate (Merck, Darmstadt, Germany) was the oxidant. Other chemicals used, including nitric acid, polyethylene glycol (PEG) 6000, glycine, urea, citric acid monohydrate, methyl orange, and Aquadest, were analytical grade and sourced from Sigma–Aldrich, Darmstadt, Germany.

### *2.2. Synthesis of $Bi_2O_3$ using the Solution Combustion Method*

$Bi_2O_3$ particles were synthesized using a modified method proposed by La et al. (2013). Thus, 2.91 g of bismuth nitrate pentahydrate was dissolved into 10 ml of 0.04 M nitric acid. Then, 0.04 g of PEG 6000 and citric acid as fuel were simultaneously added. The solution was then heated for 8 h at 300°C. The product obtained was calcined for 4 h in a furnace (Eurotherm 2116; Eurotherm, Germany) at 700°C. The same procedure was applied to the other fuels, urea and glycine, using the same molar ratio as the citric acid. The mass of each added fuel was 1.20, 1.50, and 4.20 g for urea, glycine, and citric acid, respectively.

### *2.3. Characterization*

The $Bi_2O_3$ particles' morphology was observed using 20 kV field-emission scanning electron microscopy (S-5000; Hitachi High-Technologies Corp., Tokyo, Japan). The crystal structures of the $Bi_2O_3$ particles were determined using X-ray diffraction (XRD) with a CuKα radiation source, 30 mA electric current, 30 kV voltage, and a 2θ range of 10°–90° (D2 PHASER; Bruker Corp., Billerica, MA, USA). Chemical bonding on the surface of the $Bi_2O_3$ particles was determined by Fourier Transform InfraRed (FTIR) in the range of 500–4,500 $cm^{-1}$ (Shimadzu IRAffinity-1; Shimadzu, Japan). The band gaps were determined using Diffuse Reflectance Ultraviolet-Visible Spectroscopy (DRS-UV) analysis (UV 1700 Pharma Spec; Shimadzu, Japan).

### *2.4. Photocatalytic activity*

Photocatalytic activity test was performed by adding 0.1 g of $Bi_2O_3$ to 50 mL of 5-ppm methyl-orange solution. The solution was then inserted into a photocatalysis reactor and stirred with a magnetic stirrer for time variations of 2, 4, 6, 8, and 10 h under ultraviolet-A (UV-A) light irradiation. The dye solution had also been treated without UVA light irradiation for 2 h to identify the adsorption effect. The methyl-orange degradation was measured using a UV-Vis spectrophotometer with a wavelength of 462 nm. Furthermore, the percentage of methyl-orange degradation after the photocatalytic process was determined by the Equation 1:

$$\text{degradation percentage} = \left(\frac{C_0 - C_t}{C_0}\right) \times 100\ \% \quad (1)$$

with $C_0$ is the initial concentration of methyl orange (ppm), and $C_t$ is the final concentration of methyl orange (ppm) at *t* time.

## 3. Results and Discussion

Generally, for the solution combustion method, the precursor comprises a mixture of metal nitrates, as the metal source and oxidizing agent and fuel, as the reducing agent. Metal nitrates are preferred due to the efficient oxidizing power of $NO_3^-$ groups (Bhaduri et al., 1996). In this study, bismuth nitrate pentahydrate ($Bi(NO_3)_3.5H_2O$) was used as the main precursor, and the fuel was varied: urea ($CO(NH_2)_2$), glycine ($C_2H_5NO_2$), and citric acid monohydrate ($C_6H_8O_7.H_2O$). The yield of $Bi_2O_3$ particles prepared by urea, glycine, and citric acid were 84.88%, 75.81%, and 83.52%, respectively.

The products of the solution combustion reactions before calcination are depicted in Figure 1. The colors of the obtained powders were yellowish-white, grayish-green with a slight yellow hue, and partially black with yellow for samples synthesized using urea (Figure 1a), glycine (Figure 1b), and citric acid (Figure 1c), respectively. The yellow color of all the products indicated the presence of $Bi_2O_3$. The black color in the products synthesized with either citric acid or glycine indicated the presence of carbon, as both these fuels have higher carbon content than urea.

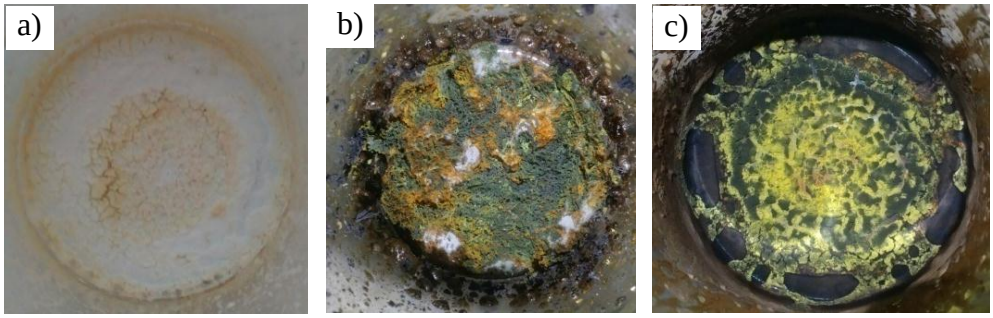


**Figure 1** Products synthesized using different fuels: (a) urea; (b) glycine; and (c) citric acid, before calcination

To confirm the formation of $Bi_2O_3$ particles, improve the crystallinity, and decompose the carbon content, calcination was carried out at 700°C for 4 h. The color of all the particles prepared using the three fuels changed to yellow after the calcination process, as depicted in Figure 2. The yellow color indicated the complete formation of $Bi_2O_3$ and the removal of carbon.


**Figure 2** $Bi_2O_3$ synthesized using a) urea, b) glycine, and c) citric acid after calcination

To further verify the formation of $Bi_2O_3$ and the decomposition of the fuel into gases, FTIR analysis was conducted. Figure 3 depicts the FTIR spectra of the particles synthesized using urea, glycine, and citric acid.

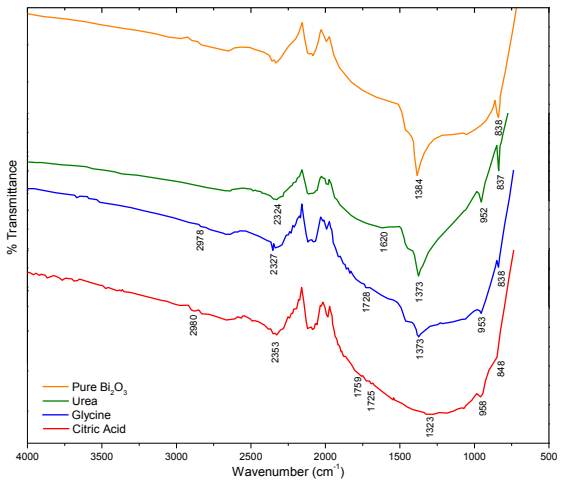


**Figure 3** FTIR spectra of pure $Bi_2O_3$ and $Bi_2O_3$ particles synthesized using urea, glycine, and citric acid

The spectra depicted the presence of peaks at 837, 838, and 848 $cm^{-1}$, which were attributed to Bi-O-Bi. Vibration modes were also observed at 1.373 and 1.323 $cm^{-1}$,

corresponding to Bi-O stretching (Bandyopadhyay and Dutta, 2017). These results indicated that $Bi_2O_3$ had been successfully formed. This was supported by the FTIR spectrum of pure $Bi_2O_3$, which showed peaks at 838 and 1.384 $cm^{-1}$. Interestingly, the vibration mode at ~2.300 $cm^{-1}$ was assigned to asymmetric stretching of $CO_2$ adsorbed on the surface (Labib, 2015) and observed in all products. The presence of $CO_2$ may have been the result of the solutions' combustion. As previously mentioned, $CO_2$ molecules are released during the formation of metal oxide powders in the solution combustion reaction. These molecules may have been trapped in the $Bi_2O_3$ or come into contact with its surface.

The FTIR spectrum of the $Bi_2O_3$ synthesized using urea exhibited a peak at 1.620 $cm^{-1}$, which indicated the existence of amine (N-H) bending, derived from the urea (Piasek and Urbanski, 1962). $Bi_2O_3$ synthesized using glycine exhibited a peak at 1.728 $cm^{-1}$, which was attributed to C=O and C=N groups (Dukali et al., 2014). The FTIR spectrum of $Bi_2O_3$ synthesized using citric acid exhibited vibrational modes at 1.725 and 1.759 $cm^{-1}$, which were assigned to C=O groups and also at 2.880 and 2.978 $cm^{-1}$, which were attributed to methylene (C-H) stretching. These functional groups were derived from the citric acid. The intensity of these peaks was very low, which indicated that most of the fuel had been decomposed.

### *3.1. Structural Analysis*

Figure 4 depicts an XRD diffractogram of the $Bi_2O_3$ particles, synthesized with the various fuels, after calcination. The $Bi_2O_3$ particles synthesized using the urea and glycine fuels were a mixture of α-$Bi_2O_3$ (monoclinic) and β-$Bi_2O_3$ (tetragonal) phases. The $Bi_2O_3$ particles synthesized using the citric acid fuel were α-$Bi_2O_3$ (monoclinic) in phase. The presence of α-$Bi_2O_3$ was characterized by the highest three peaks for $Bi_2O_3$ at 2θ for the particles prepared with urea (27.7, 33.3, 27.2), glycine (27.8, 33.4, 27.3), and citric acid (27.892, 33.544, 27.412). The presence of β-$Bi_2O_3$ was characterized by peaks for $Bi_2O_3$ at 2θ of 30.478, 41.768, 45.420 and 30.565, 41.854, 45.505 for particles prepared using urea and glycine, respectively. The peaks corresponding to α-$Bi_2O_3$ and β-$Bi_2O_3$ were assigned using the Joint Committee on Powder Diffraction Standards (JCPDS) database 41-1449 and 27-0050 files, respectively.

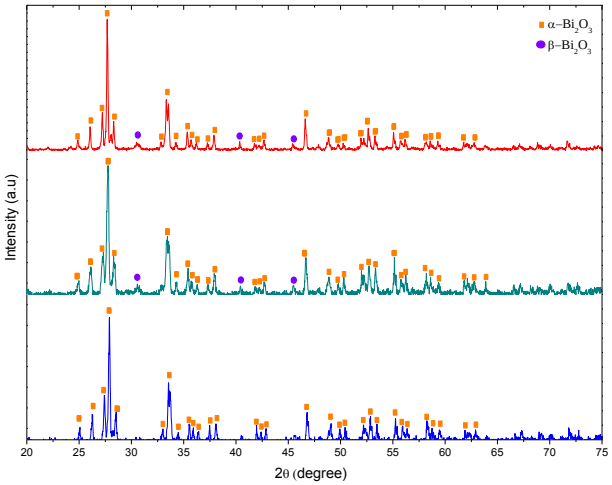


**Figure 4** XRD diffractograms of $Bi_2O_3$ particles synthesized using: (a) urea; (b) glycine; and (c) citric acid after calcination

The α-$Bi_2O_3$ phase was dominant in all products, as depicted in Figure 4. The $Bi_2O_3$ particles tended to return to the α-$Bi_2O_3$ phase during the cooling process because this phase is more stable than the other $Bi_2O_3$ polymorphs at room temperature (La et al., 2013). However, minor amounts of β-$Bi_2O_3$ phase might be formed in $Bi_2O_3$ particles synthesized

using urea and glycine, as they are reactive fuels and release a large amount of energy during the combustion reaction. Calcination at 700°C also promotes the formation of β-$Bi_2O_3$ phase (La et al., 2013) and, as reported by Jalalah et al. (2015), the β-$Bi_2O_3$ phase is formed at approximately 650°C.

Figure 5 depicts the morphology of $Bi_2O_3$ prepared using various fuels. Before calcination, $Bi_2O_3$ prepared with urea and citric acid formed dense particles with thin, flake-like and bulky, thick, flake-like structures, as depicted in Figures 5a and 5c, respectively. Conversely, the addition of glycine resulted in a porous material, formed by the agglomerated nanoparticles, as depicted in Figure 5b. Urea was expected to generate bulky, thick $Bi_2O_3$ particles because it contains the highest number of amine groups, which promote an exothermic reaction when in contact with nitrate. This reaction provided the high energy required for the $Bi_2O_3$ formation. The different results obtained herein may have been due to the products' different fuel to oxidant ratios. Generally, in addition to fuel type, the ratio of fuel to oxidant ($\Phi$) and the pre- and post-treatment temperatures will also affect the particles' morphologies. Even though the molar ratios of the precursors were the same, the molar ratios of the fuels to the oxidants were different. This occurred because of the differences in the reducing and oxidizing valence ratio$\left(\frac{RV}{OV}\right)$ (Li et al., 2015). The ratios of fuel to oxidant for urea, glycine, and citric acid were 1.3, 2.0, and 4.0, respectively. According to the theory of chemical propellants, maximum energy will be released when the reaction is in the stoichiometric state ($\Phi = 1$), while a fuel-rich condition ($\Phi > 1$) results in incomplete combustion. To achieve complete combustion, a supply of oxygen is required (Li et al., 2015). In this study, the combustion reaction was carried out in an open chamber at 300°C, so the molecular oxygen in the atmosphere may have contributed to the combustion process. Subsequently, the combustion reaction in citric acid, used as the fuel, led to greater crystal growth and bigger crystallites compared to the other fuels.

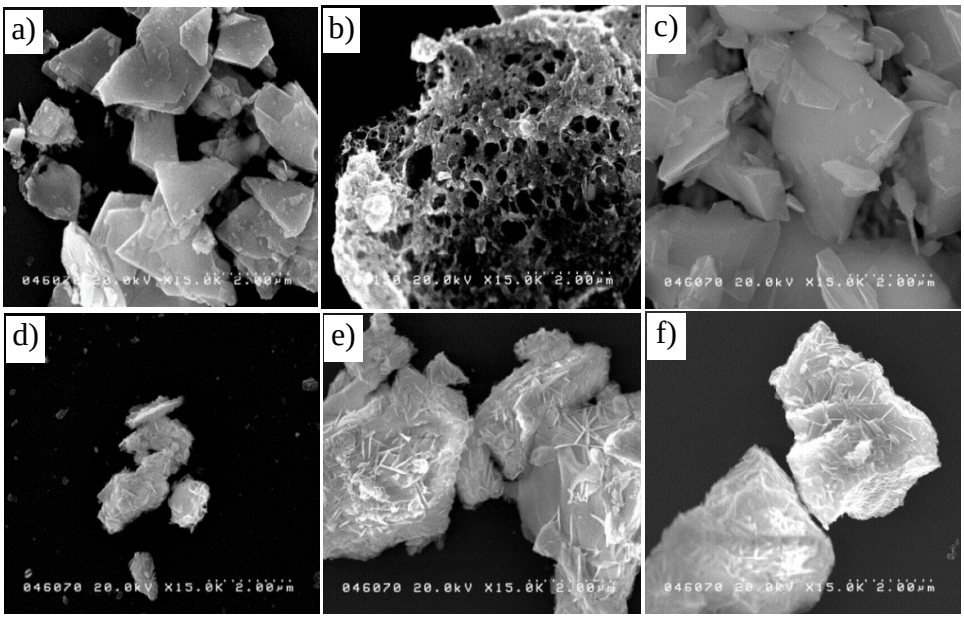


**Figure 5** Scanning electron microscopy (SEM) images of $Bi_2O_3$ before (a, b, c) and after calcination (d, e, f) prepared with urea, glycine, and citric acid, respectively

Figures 5d, 5e, 5f show that the calcination step led to crystal growth and the formation of rod-like $Bi_2O_3$ particles, prepared using urea, as depicted in Figure S1. However, the crystal growth on the $Bi_2O_3$ prepared using glycine was long asterisk-shaped, as depicted in Figures 5e and S2c. Here, the main particles retained a porous structure. Figures 5f and S3 show that the $Bi_2O_3$ particles prepared with citric acid exhibited crystal growth in the

form of rods and the main particles tended to sinter. The rod-like structures may have resulted from the growth of tetragonal crystal structures. The XRD diffractograms, depicted in Figure 4, confirmed the formation of this crystal structure even at low intensities.

*3.2. Photocatalytic Activity*

The photocatalytic activity of the prepared $Bi_2O_3$ particles was evaluated using methyl orange as the dye organic material. Figure 6 shows that the photocatalytic activity of the $Bi_2O_3$ particles synthesized using citric acid was lower than that of the particles prepared using glycine and urea. These results were supported by the diffuse reflectance spectroscopy-ultraviolet (DRS-UV) analysis, depicted in Figure 7, where particles prepared with citric acid had higher band gap energy (2.75 eV) than those prepared with glycine (2.3 eV) and urea (2.55 eV). The larger the material's band gap, the more difficult it is for the electrons to excite from the valence band to the conduction band, thereby decreasing the photocatalytic performance. A band gap of 2.75 eV is in accordance with the band gap energy of α-$Bi_2O_3$ (Iyyapushpam et al., 2013). Additionally, the energy band gaps of 2.55 and 2.30 eV were in agreement with the band gap energy of β-$Bi_2O_3$ (Ali, 2014). Both $Bi_2O_3$ polymorphs exhibited higher photocatalytic activity than other $Bi_2O_3$ polymorphs (Zhou et al., 2011). In addition to the value of the band gap energy, the lowest photocatalytic activity of $Bi_2O_3$ particles, prepared by citric acid, may have been due to the dominant content of α-$Bi_2O_3$, as depicted in the XRD diffractogram result illustrated in Figure 4c. It has been reported that the combination of α- and β-$Bi_2O_3$ phases significantly improves the photocatalytic degradation of a methyl-orange solution compared to one phase alone (Hou et al., 2013).

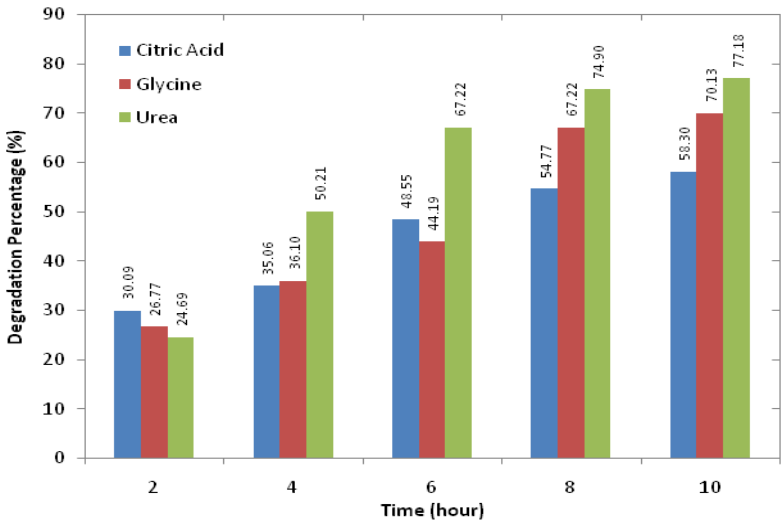


**Figure 6** Percentage of methyl-orange degradation after photocatalysis with $Bi_2O_3$ synthesized using different fuels

The degradation kinetics of methyl orange by $Bi_2O_3$ particles, prepared using the various fuels, was also studied.

Generally, the dye's degradation by photocatalyst activity followed first-order kinetics, as expressed by the Equation 2:

$$ln\ C_t = ln\ C_0 - kt \quad (2)$$

where, $C_0$ is the initial concentration of the methyl-orange solution (ppm), $C_t$ is the concentration of the methyl orange solution (ppm) at time t, and $k$ is the constant of the degradation rate at first order ($s^{-1}$).

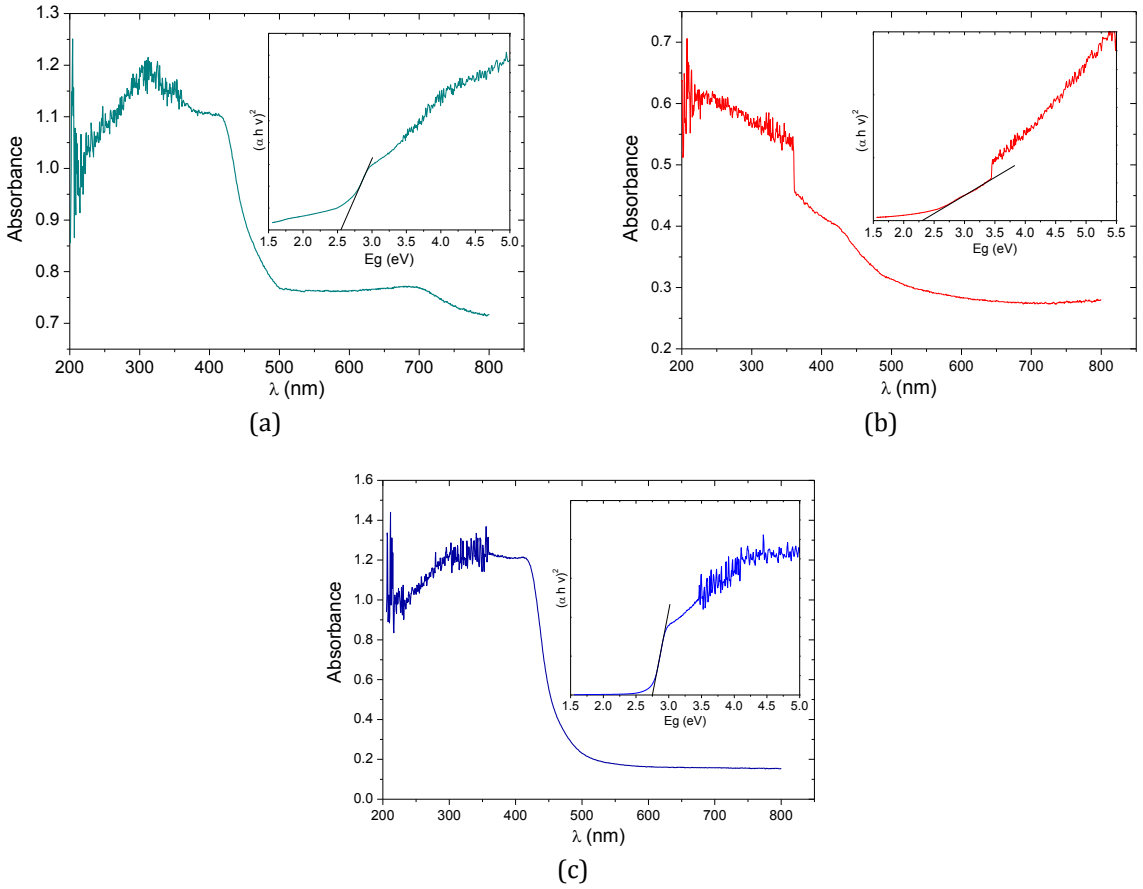


**Figure 7** DRS-UV spectra of $Bi_2O_3$ synthesized using: (a) urea; (b) glycine; and (c) citric acid

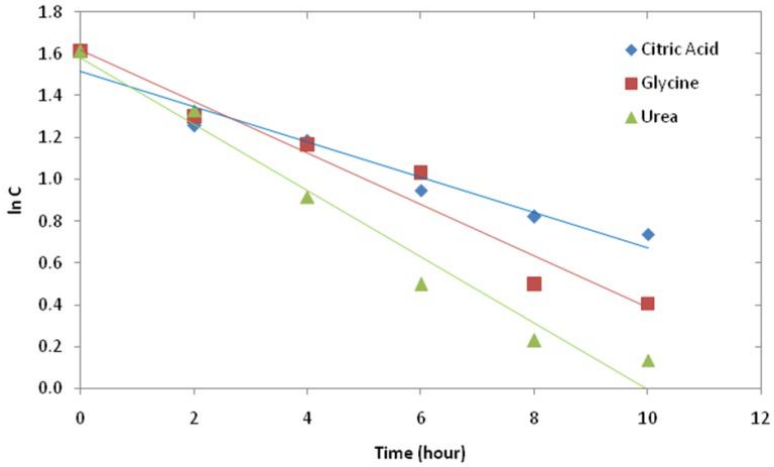


**Figure 8** First-order reaction of methyl-orange degradation by $Bi_2O_3$, synthesized using different fuels

Figure 8 depicts the degradation of the methyl orange following a first-order reaction. The methyl-orange degradation rate constants of $Bi_2O_3$ synthesized using urea, glycine, and citric acid were $4.38\times10^{-5}$ $s^{-1}$, $3.38\times10^{-5}$ $s^{-1}$, and $2.33\times10^{-5}$ $s^{-1}$, respectively. Thus, it was concluded that $Bi_2O_3$ synthesized using urea provided the highest methyl-orange degradation kinetic. It was confirmed that the physicochemical properties of $Bi_2O_3$

synthesized using different fuels highly affected the photocatalytic activity. Particles prepared with urea had the lowest band gap and therefore, became the most active catalysts.

## 4. Conclusions

$Bi_2O_3$ particles were successfully synthesized using the solution combustion method with various fuels: urea, glycine, and citric acid. The successful synthesis was confirmed by the particles' yellow color and the presence of a Bi-O-Bi vibration mode at 837–848 $cm^{-1}$ by FTIR analysis. The different fuels affected the morphology and physical properties of the synthesized particles. α-$Bi_2O_3$ (monoclinic), identified at 2θ 27.2, 27.7 and 33.3, was observed to be the major phase in all the prepared particles; however, samples synthesized using urea and glycine exhibited a minor presence of β-$Bi_2O_3$ (tetragonal), observed at 2θ 30.5, 41.8, 45.5. Different morphological structures of $Bi_2O_3$ particles were found, including thin-flake, porous, and bulky flake-like structures, which were observed in the particles prepared using urea, glycine, and citric acid, respectively. The effect of the fuels was also indicated by the particles' band gap energies, namely 2.55 eV, 2.3 eV, and 2.75 eV for those prepared with urea, glycine, and citric acid, respectively. Furthermore, the highest photocatalytic activity for the degradation of methyl orange was exhibited by $Bi_2O_3$ particles synthesized using urea, followed by glycine and citric acid, with degradation rate constants of $4.38\times10^{-5}$ $s^{-1}$, $3.38\times10^{-5}$ $s^{-1}$, and $2.33\times10^{-5}$ $s^{-1}$, respectively.

## Acknowledgements

The authors wish to acknowledge the Ministry of Research, Technology and Higher Education, Republic of Indonesia, for its financial support through a *Penelitian Hibah Kompetensi (HiKom)* grant, 2018, with the grant no. 101-71/UN7.P4.3/PP/2018. Moreover, Yayuk Astuti would like to thank Diponegoro University for financial support during the Postdoctoral/Sabbatical Program, 2017, with the grant no. 990/UN7.P/HK/2017, and the Thermal Fluid Lab, Chemical Engineering, Hiroshima University for the use of its SEM instrument facility.

## References

Ali, R.S., 2014. Structural and Optical Properties of Nanostructured Bismuth Oxide. *International Letters of Chemistry, Physics and Astronomy,* Volume 34, pp. 64–72

Astuti, Y., Arnelli, A., Pardoyo, P., Fauziyah, A., Nurhayati, S., Wulansari, A.D., Andianingrum, R., Widiyandari, H., Bhaduri, G.A., 2017. Studying Impact of Different Precipitating Agents on Crystal Structure, Morphology and Photocatalytic Activity of Bismuth Oxide. *Bulletin of Chemical Reaction Engineering & Catalysis,* Volume 12(3), pp. 478–484

Astuti, Y., Fauziyah, A., Widiyandari, H., Widodo, D., 2019. Studying Impact of Citric Acid-Bismuth Nitrate Pentahydrate Ratio on Photocatalytic Activity of Bismuth Oxide Prepared by Solution Combustion Method. *Rasayan Journal of Chemistry,* Volume 12(4), pp. 2210–2217

Bandyopadhyay, S., Dutta, A., 2017. Thermal, Optical and Dielectric Properties of Phase Stabilized δ–Dy-$Bi_2O_3$ Ionic Conductors. *Journal of Physics and Chemistry of Solids,* Volume 102, pp. 12–20

Bedoya Hincapie, C.M., Pinzon Cardenas, M.J., Orjuela, A., Edgar, J., Restrepo Parra, E., Olaya Florez, J.J., 2012. Physical-Chemical Properties of Bismuth and Bismuth Oxides: Synthesis, Characterization and Applications. *Dyna,* Volume 79(176), pp. 139–148

Bhaduri, S., Zhou, E., Bhaduri, S., 1996. Auto Ignition Processing of Nanocrystalline α-$Al_2O_3$. *Nanostructured Materials,* Volume 7(5), pp. 487–496

Cheng, L., Kang, Y., 2015. $Bi_5O_7I/Bi_2O_3$ Composite Photocatalyst with Enhanced Visible Light Photocatalytic Activity. *Catalysis Communications,* Volume 72, pp. 16–19

Dukali, R.M., Radović, I.M., Stojanović, D.B., Šević, D.D., Radojević, V.J., Jocić, D.M., Aleksić, R.R., 2014. Electrospinning of Laser Dye Rhodamine B-doped Poly (Methyl Methacrylate) Nanofibers. *Journal of the Serbian Chemical Society,* Volume 79(7), pp. 867–880

Gotić, M., Popović, S., Musić, S. 2007. Influence of Synthesis Procedure on the Morphology of Bismuth Oxide Particles. *Materials Letters,* Volume 61(3), pp. 709–714

Hashimoto, T., Ohta, H., Nasu, H., Ishihara, A., 2016. Preparation and Photocatalytic Activity of Porous $Bi_2O_3$ Polymorphisms. *International Journal of Hydrogen Energy,* Volume 41(18), pp. 7388–7392

Hou, J., Yang, C., Wang, Z., Zhou, W., Jiao, S., Zhu, H., 2013. In Situ Synthesis of α–β Phase Heterojunction on $Bi_2O_3$ Nanowires with Exceptional Visible-light Photocatalytic Performance. *Applied Catalysis B: Environmental,* Volume 142-143, pp. 504–511

Iyyapushpam, S., Nishanthi, S., Padiyan, D.P., 2013. Photocatalytic Degradation of Methyl Orange using α-$Bi_2O_3$ Prepared without Surfactant. *Journal of Alloys and Compounds,* Volume 563, pp. 104–107

Jalalah, M., Faisal, M., Bouzid, H., Park, J.-G., Al-Sayari, S., Ismail, A.A. 2015a. Comparative Study on Photocatalytic Performances of Crystalline α-and β-$Bi_2O_3$ Nanoparticles under Visible Light. *Journal of Industrial and Engineering Chemistry,* Volume 30, pp. 183–189

La, J., Huang, Y., Luo, G., Lai, J., Liu, C., Chu, G., 2013. Synthesis of Bismuth Oxide Nanoparticles by Solution Combustion Method. *Particulate Science and Technology,* Volume 31(3), pp. 287–290

Labib, S., 2015. Preparation, Characterization and Photocatalytic Properties of Doped and Undoped $Bi_2O_3$. *Journal of Saudi Chemical Society*, Volume 21(6), pp. 664–672

Lackner, M., 2010. *Combustion Synthesis: Novel Routes to Novel Materials*. Austria: Bentham Science Publishers

Li, F.-T., Ran, J., Jaroniec, M., Qiao, S.Z., 2015. Solution Combustion Synthesis of Metal Oxide Nanomaterials for Energy Storage and Conversion. *Nanoscale,* Volume 7(42), pp. 17590–17610

Liu, L., Jiang, J., Jin, S., Xia, Z., Tang, M., 2011. Hydrothermal Synthesis of β-Bismuth Oxide Nanowires from Particles. *CrystEngComm,* Volume 13(7), pp. 2529–2532

Mallahi, M., Shokuhfar, A., Vaezi, M., Esmaeilirad, A., Mazinani, V., 2014. Synthesis and Characterization of Bismuth Oxide Nanoparticles via Sol-Gel Method. *American Journal of Engineering Research,* Volume 3(4), pp. 162–165

Piasek, Z., Urbanski, T., 1962. The Infra-red Absorption Spectrum and Structure of Urea. *Bulletin De L'Academie Polonaise Des Sciences: Serie Des Sciences Chimiques,* Volume X(3), pp. 113–120

Rahman, A., Nurjayadi, M., Wartilah, R., Kusrini, E., Prasetyanto, E.A., Degermenci, V., 2018. Enhanced Activity of $TiO_2$/Natural Zeolite Composite for Degradation of Methyl Orange under Visible Light Irradiation. *International Journal of Technology*, Volume 9(6), pp. 1159–1167

Rasouli, S., Oshani, F., Hashemi, S., 2011. Effect of Various Fuels on Structure and Photo-catalytic Activity of Nanocrystalline $TiO_2$ Prepared by Microwave-assisted Combustion Method. *Progress in Color, Colorants and Coatings,* Volume 4(2), pp. 85–94

Raveendra, R., Prashanth, P., Nagabhushana, B., 2016. Study on the Effect of Fuels on Phase Formation and Morphology of Combustion Derived α-$Al_2O_3$ and NiO Nanomaterials. *Advanced Materials Letters,* Volume 7(3), pp. 216–220

Winatapura, D.S., Dewi, S.H., Adi, W.A., 2016. Synthesis, Characterization, and Photocatalytic Activity of $Fe_3O_4$@ ZnO Nanocomposite. *International Journal of Technology*, Volume 7(3), pp. 408–416

Zhou, B., Huang, Q., Zhang, S., Cai, C., 2011. β-and α-$Bi_2O_3$ Nanoparticles Synthesized via Microwave-assisted Method and Their Photocatalytic Activity Towards the Degradation of Rhodamine B. *Materials Letters,* Volume 65(6), pp. 988–990